

Facet-dependent Catalysis of CuNi Nanocatalysts toward 4–Nitrophenol Reduction Reaction

Can Li¹, Yiliang Luan¹, Bo Zhao², Amar Kumbhar³, Xiaobo Chen⁴, David Collins⁵, Guangwen Zhou⁴, Jiye Fang^{1,4*}

¹Department of Chemistry, State University of New York at Binghamton, New York, USA.

²College of Arts & Sciences Microscopy, Texas Tech University, Texas, USA.

³Chapel Hill Analytical and Nanofabrication Laboratory, University of North Carolina at Chapel Hill, North Carolina, USA.

⁴Materials Science and Engineering Program, State University of New York at Binghamton, New York, USA.

⁵Department of Geological Sciences and Environmental Studies, State University of New York at Binghamton, New York, USA.

ABSTRACT

We report a facile method to fabricate CuNi nano-octahedra and nanocubes using a colloidal synthesis approach. The CuNi nanocrystals terminated with exclusive crystallographic facets were controlled and achieved by a group of synergetic capping ligands in a hot solution system. Specifically, the growth of {111}-bounded CuNi nano-octahedra is derived by a thermodynamic control, whereas the generation of {100}-terminated CuNi nanocubes is steered by a kinetic capping of chloride. Using a reduction of 4-nitrophenol with sodium borohydride as a model reaction, CuNi nano-octahedra and nanocubes demonstrated a strong facet-dependence due to their different surface energies although both exhibited remarkable catalytic activity with the high rate constant over mass (k/m). A kinetic study indicated that this is a pseudo first-order reaction with an excess of sodium borohydride. CuNi nanocubes as the catalysts showed better catalytic performance (k/m = $385 \text{ s}^{-1} \cdot \text{g}^{-1}$) than the CuNi nanocuthedra (k/m = $120 \text{ s}^{-1} \cdot \text{g}^{-1}$), indicating that 4-nitrophenol and hydrogen were adsorbed on the {100} facets with their molecules parallel to the surface much easier than those on {111} facets.



INTRODUCTION

Bimetallic nano-alloys have attracted growing interest due to their unique catalytic performance including high activity, sensitive selectivity, and excellent durability. These outstanding catalytic characters rely on their surface structures, size, shape, and composition[1-6]. High-performance nanocatalysts have been developed using many strategies in terms of their tuneable ligand effect, geometric effect, and shape effect. Among these, the shape-effect of nanocatalysts with exclusively exposed facets has drawn increased attention for the development of catalytic selectivity and activity, and the relevant applications to electrochemical reactions, small organic molecular reactions including hydrogenation and reduction reaction have been reported[7-11].

The previous study has demonstrated that CuNi nano-octahedra in different sizes, such as 10 nm and 20 nm, can be synthesized from a colloidal system and exhibited different performances toward 4-nitrophenol (4-NP) reduction reaction[12]. In addition, all of the {111}-terminated CuNi nano-octahedra show higher activities in comparison with spherical CuNi nanoalloys, indicating that {111} facets exposed from the nano-octahedra are superior to polycrystalline surfaces presented on the spherical nanoalloys toward the 4-NP reduction reaction. In order to investigate the catalytic contribution from the {111} and {100} facets, in this work, we comparably prepare nano-octahedra and CuNi nanocubes using different synthesis strategies and explore their individual performances toward 4-NP reduction reaction under the same conditions. We also have an interest in determining whether or not 4-NP reduction is a catalyst facet-dependent reaction.

EXPERIMENT

Synthesis and characterization of CuNi bimetallic nano-octahedra and nanocubes

20 nm CuNi nano-octahedra were prepared using a modified synthetic method as reported previously [12,13]. Typically, a borane morpholine (BM, Alfa Aesar, 95%) solution as a reducing agent was prepared using the following recipe: 0.1816 g of BM pellets were introduced into a degassed mixture (vide infra) containing 2.50 mL of diphenyl ether (DPE, Sigma-Aldrich, 99%), 1.70 mL of oleylamine (OAm, Sigma-Aldrich, 70%) and 0.34 mL of oleic acid (OA, Sigma-Aldrich, 90%). In another flask, 0.05 mmol of cupric(II) acetylacetonate (Chem Implex Int., >98%) and 0.05 mmol of nickel (II) acetylacetonate (Alfa Aesar, 95%) were added in a mixture consisting of 5.00 mL of DPE, 3.40 mL of OAm and 0.68 mL of OA, generating a crystal blue solution after all solids were dissolved. After a degassing treatment under vacuum at 90 °C, this Cu/Ni-colloidal mixture was quickly heated to 240 °C under argon protection, followed by an injection of the freshly prepared BM solution (0.50 mL), forming a dark brown mixture rapidly. This mixture was further evolved for another 30 min at 240 °C before the isolation. The product was collected by centrifugation and purified twice using a pair of solvents (hexane and ethanol). Finally, the CuNi nano-octahedra were re-dispersed into hexane to form suspensions under argon protection.

To synthesize 20 nm CuNi nanocubes, 0.05 mmol of copper (I) chloride (CuCl, Alfa Aesar, 99.999%) and 0.05 mmole of nickel (II) chloride (NiCl₂, Alfa Aesar, 98%) were used as the metal precursors. The rest chemicals, including BM solution, DPE, OAm as well as OA, and the synthetic procedure/recipe are similar to those of 20 nm CuNi nano-octahedra, respectively.

nttps://doi.org/10.1557/adv.2020.5

The morphology and composition of as-prepared catalysts were further characterized by inductively coupled plasma-optical emission spectrometry (ICP-OES), X-ray diffraction (XRD), and transmission electron microscope (TEM).

Catalytic activity evaluation of 4-NP reduction reaction

The as-prepared CuNi nano-octahedra and nanocubes were loaded onto carbon black (Vulcan xc72) with a total metal fraction of 50 wt%, respectively, using a procedure reported previously[6]. Both catalysts (denoted as CuNi nano-octahedra/C and CuNi nano-cubes/C) were re-dispersed into ethanol after a sufficient ultra-sonication manipulation. The concentration of the catalyst suspensions (including the carbon black support) was determined as 1.0 mg/mL.

In a typical experiment of 4-NP reduction reaction, 0.8 mmol (30.6 mg) of sodium borohydride (NaBH₄, Sigma-Aldrich, 99%) was dissolved into 8.0 mL of ultrapure water (18.2 M Ω ·cm) in an ice-water bath[12]. 40.0 μ L of the as-prepared catalyst suspensions were introduced into this vigorously stirred solution, followed by a rapid injection of 4-NP (Sigma-Aldrich, >99%) aqueous solution (300 μ L, 10 mmol/L). The progress of 4-NP reduction was monitored by checking the Ultraviolet/visible (UV/Vis) absorption spectra of the reaction mixture (10-time dilution). By applying Lamber-Beer's Law, A_t/A_θ was converted into the retained concentration (C_t) of 4-NP, where A_t and A_θ represent the absorbance at 400 nm at a specific time and the initial time, respectively. Consequently, the apparent rate constants (k) for a pseudo first-order reaction with different amounts of catalysts can be obtained from the slope of the $lnC_t - t$ plot and the k/m ($s^{-1} \cdot g^{-1}$) can be further calculated.

RESULTS AND DISCUSSION

Morphology-controlled synthesis of CuNi NCs

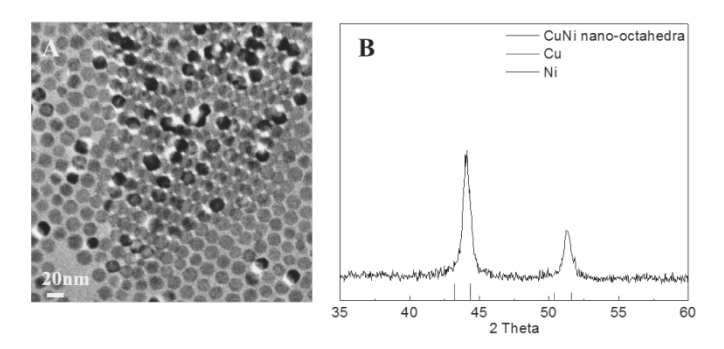


Figure 1. TEM image (A) and XRD pattern (B) of 20 nm CuNi nano-octahedra. The red and blue lines on the bottom of (B) show standard XRD patterns of Cu and Ni (ICDD PDF cards 00-001-1241, 00-001-1258), respectively.

To prepare the CuNi nano-octahedra, a facile synthesis method was utilized according to the previous study[12]. In this work, the particle size of the as-prepared CuNi nano-octahedra was determined as 20 ± 1 nm, based on the TEM characterization (Figure 1). The nucleation kinetics plays a key role in the size control once BM is

nttps://doi.org/10.1557/adv.2020.5

introduced into the system at a high temperature (240 °C). Since the {111} facets generally possess lower surface energy compared with the {100} facets for fcc metals[14,15], it is believed that the growth of CuNi nano-octahedra is thermodynamically favorable in this colloidal system. As shown in Figure 1(B), the (111) and (200) XRD peaks of the 20 nm CuNi nano-octahedra are within the range of corresponding (111) and (200) peaks of the standard Cu and Ni, respectively, indicating a formation of Cu-Ni alloy rather than individual Cu or Ni component. ICP-OES technique was used to further analyze the elemental composition, showing a bulk composition of Cu₄₉Ni₅₁, which is considered an almost equal molar ratio between Cu and Ni precursors. In addition, the intensity ratio between (111) and (200) peaks in Figure 1 (B) is apparently higher than that from the standard XRD patterns (~2.6 vs 2.0), indicating the existence of {111}-faceting layer in this XRD sample. This means that most of the {111} facets are perfectly orientated, and therefore the diffraction intensity of (111) is dramatically enhanced.

The synthetic protocol of CuNi nanocubes is similar to that of CuNi nanooctahedra, except for the difference of metal precursors. As mentioned above, the Cl as a capping ligand induces the formation of CuNi nanocubes with exclusive {100} facets. In our case, the Cl⁻ in the colloidal system serves as a strong capping agent on {100} facets during the growth stage. After the Cu-Ni seeds boom in the nucleation stage, the residues of the Cu and Ni ions can be gradually reduced and selectively deposited onto those non-{100} facets since the {100} facets are meanwhile covered by Cl. This kind of growth leads to a vanishing of the non-{100} facets, resulting in {100}-bounded CuNi cubes. We have replaced the metal chlorides with bromide precursors, CuBr (Stream Chemicals, 98%) and NiBr₂ (Alfa Aesar, 99%), and investigated the binding effect of the bromides. We determined that these bromide precursors yield CuNi nano-polyhedra only instead of nanocubes under similar synthetic conditions. This indicates that the bromide ligands possess less capping capability on (100) facets compared with the chloride counterpart. The TEM image of the as-prepared CuNi nanocrystals shown in Figure 2 (A) confirmed the hypothesized shape, demonstrating a cubic morphology with an average size of 20 nm. ICP-OES analysis suggests that the composition of the as-prepared nanocubes is $Cu_{53}Ni_{47}$, which is assumed to close to Cu:Ni = 1:1. In the XRD pattern shown in Figure 2(B), the {111} and {200} peaks of CuNi nanocubes show up in the range of the corresponding peaks of the pure Cu and Ni, respectively, supporting the alloy phase in the harvested products.

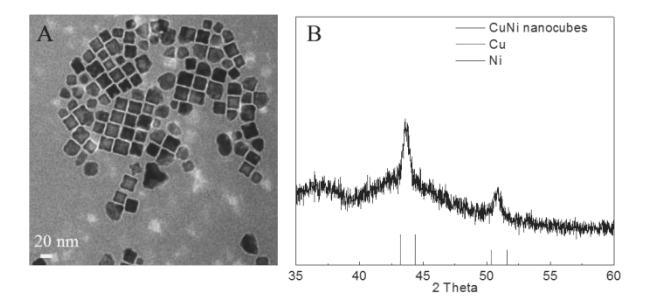


Figure 2. TEM images (A) and XRD pattern (B) of 20 nm CuNi nanocubes. The red and blue lines on the bottom of (B) show standard XRD patterns of Cu and Ni (ICDD PDF cards 00-001-1241, 00-001-1258), respectively.

Shape-effect toward catalytic performance

To evaluate the shape effect of CuNi nano-alloys toward catalytic performance, the 4-NP reduction reaction was adopted to determine the different activities of catalysts in diverse shapes. The conversion of toxic 4-NP into less toxic 4-aminophenol is a meaningful way in drug manufacturing design. In our case, excessive NaBH₄ was used as the reducing agent and UV/Vis absorption spectra were recorded to monitor the reaction progress. As illustrated in Figure 3, the highest absorption peaks at a wavelength of 400 nm in both UV/Vis absorption spectra (Figure 3A and 3B) are ascribed to the absorption of 4-NP. Without adding the catalysts, this peak remained unchanged even elapsing for 1 hour, indicating that no reduction took place. When a certain amount of the as-prepared catalysts (CuNi nano-octahedra/C and CuNi nanocubes/C) were injected into the reaction system, the intensity of the 4-NP absorption peak gradually decreased as the reaction proceeded in a short period of time. Since the NaBH₄ used in this reaction greatly exceeded the stoichiometric equivalent compared to the 4-NP, NaBH₄ was assumed as a constant within a span of the short reaction period and the 4-NP was treated as a limiting reagent. Thus, pseudo first-order kinetics to 4-NP reduction is applied to the cast in order to determine the apparent rate constant (k). As a result (shown in Figure 3C and 3D), the 20 nm CuNi nanocubes/C exhibited a k value of 0.0077 s^{-1} and a k/m value of 385 $s^{-1} \cdot g^{-1}$, whereas the 20 nm CuNi nano-octahedra/C gave a k value of 0.0048 s⁻¹ and a k/m value of 120 s⁻¹·g⁻¹. This result suggests that the CuNi nanocubes/C possess a higher catalytic activity in the 4-NP reduction reaction. It is believed that the {100} CuNi facets that are dominant surfaces in the cubic nano-catalysts could easily adsorb some reactants such as 4-NP and H₂ through a parallel configuration between the molecules and the catalyst surface, in contrast to their counterparts, the {111} facets. This leads to fast 4-NP reduction kinetics in the case of CuNi nanocubes.

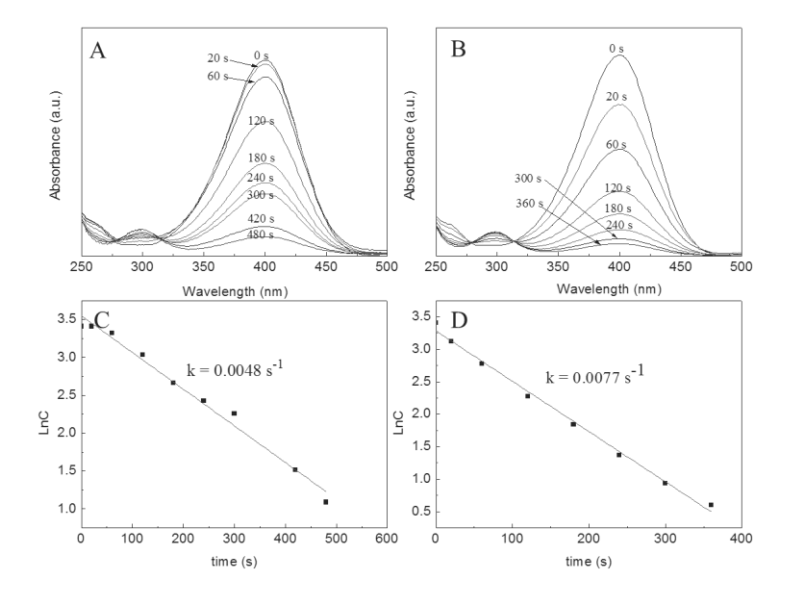


Figure 3. Time-resolved UV/Vis absorption spectra of 4-NP reduction by NaBH4 in the presence of (A) 20 nm CuNi nano-octahedra/C and (B) 20 nm CuNi nanocubes/C. A linear relationship between the logarithmic concentration of 4-NP and the time with a rate constant k obtained from the slope in the presence of (C) 20 nm CuNi nano-octahedra/C and (D) 20 nm CuNi nanocubes/C.

CONCLUSIONS

In summary, CuNi nanocubes and nano-octahedra were synthesized using a colloidal system. Different types of precursors were employed to tune the CuNi shape through different growth mechanisms. In terms of the 4-NP reduction as a model reaction, a strong catalyst facet-dependent performance was determined. The study shows that $\{100\}$ -terminated CuNi nanocubes demonstrate much higher catalytic activity ($k/m = 385 \text{ s}^{-1} \cdot \text{g}^{-1}$) than $\{111\}$ -bounded CuNi nano-octahedra ($k/m = 120 \text{ s}^{-1} \cdot \text{g}^{-1}$), indicating that 4-NP and H_2 could be easily adsorbed on the $\{100\}$ facets than the $\{111\}$ facets.

ACKNOWLEDGMENTS

This work was primarily supported by NSF (DMR-1808383). The synthesis materials were partially supported by ACS PRF (58196-ND10), and part of the TEM characterization was supported by S3IP, State University of New York at Binghamton. C.L. was partially supported by the Center for Alkaline-Based Energy Solutions, an Energy Frontier Research Center program supported by the U.S. Department of Energy, under Grant DE-SC0019445. X.C. and G.Z. acknowledge the support from the U.S. Department of Energy, Office of Basic Energy Sciences, Division of Materials Sciences and Engineering under Award No. DE-SC0001135. C.L. also thanks Dr. In-Tae Bae and John L. Grazul for their TEM training and assistance. We are grateful to Professor David M. Jenkins in the Department of Geological Sciences and Environmental Studies, State University of New York at Binghamton, for the support of XRD characterization.

REFERENCES

- 1. J. Zhang and J. Fang. J. Am. Chem. Soc. 131, 18543-18547 (2009).
- 2. J. Zhang, H. Yang, J. Fang and S. Zou. *Nano Lett.* 10, 638-644 (2010).
- J. Zhang, H. Yang, B. Martens, Z. Luo, D. Xu, Y. Wang, S. Zou and J. Fang. Chem. Sci. 3, 3302-3306 (2012).
- D. Xu, Z. Liu, H. Yang, Q. Liu, J. Zhang, J. Fang, S. Zou and K. Sun. Angew. Chem. Int. Ed. 48, 4217-4221 (2009).
- J. Zhang, Z. Luo, B. Martens, Z. Quan, A. Kumbhar, N. Porter, Y. Wang, D.-M. Smilgies and J. Fang. J. Am. Chem. Soc. 134, 14043-14049 (2012).
- C. Wang, C. Lin, B. Zhao, L. Zhang, A. Kumbhar, G. Fan, K. Sun, J. Zhang, S. Chen and J. Fang. ChemNanoMat 1, 331-337 (2015).
- 7. N.S. Porter, H. Wu, Z. Quan and J. Fang. Acc. Chem. Res. 46, 1867-1877 (2013).
 - Y. Luan, L. Zhang, C. Wang, J. Liu and J. Fang. MRS Adv. 3, 943-948 (2018).
- 9. Y. Luan, C. Li, B. Zhao, A. Kumbhar, J. Zhang and J. Fang. MRS Adv. 4, 1377-1382 (2019).
- 10. H. Guo, Y. Chen, H. Ping, J. Jin and D.-L. Peng. Nanoscale 5, 2394-2402 (2013).
- 11. J. Liu, Y. Zheng and S. Hou. *RSC Adv.* 7, 37823-37829 (2017).
- 12. C. Li, Y. Luan, B. Zhao, A. Kumbhar and J. Fang. MRS Adv. 4, 263-269 (2019).
- M. Wang, L. Wang, H. Li, W. Du, M.U. Khan, S. Zhao, C. Ma, Z. Li and J. Zeng. J. Am. Chem. Soc. 137, 14027-14030 (2015).
- 14. K.D. Gilroy, A. Ruditskiy, H.-C. Peng, D. Qin and Y. Xia. Chem. Rev. 116, 10414-10472 (2016).
- 15. L. Vitos, A.V. Ruban, H.L. Skriver and J. Kollár. Surf. Sci. 411, 186-202 (1998).